SCIENCE CHINA
Physics, Mechanics & Astronomy

• Article •

August 2012 Vol.55 No.8: 1431–1438
doi: 10.1007/s11433-012-4793-7

Numerical study of thermal history in laser aided direct metal deposition process

ZHANG YongJie, YU Gang* & HE XiuLi

Institute of Mechanics, Chinese Academy of Sciences, Beijing 100190, China

Received July 19, 2011; accepted February 13, 2012; published online June 20, 2012

Temperature evolution in the laser aided direct metal deposition (LADMD) process has considerable influence on the microstructure and properties of the final part. A 3D transient finite element model was developed to study the temperature evolution during the multilayer LADMD process. To make the property analysis from thermal history easier, a critical temperature specific to thermal history was defined and the distribution of it in the part was also discussed. The simulation results indicated that the critical temperature can make the property analysis from thermal history easier. Thermal history of all the deposited materials was similar. It was also concluded that process parameters needed to be time-varying according to the real-time temperature field during the process.

laser-aided direct metal deposition, finite element modeling, thermal history

PACS number(s): 42.62.Cf, 44.05.+e

Citation: Zhang Y J, Yu G, He X L. Numerical study of thermal history in laser aided direct metal deposition process. Sci China-Phys Mech Astron, 2012, 55: 1431–1438, doi: 10.1007/s11433-012-4793-7

1 Introduction

Laser aided direct metal deposition (LADMD) technology is a modern rapid manufacturing technology which is similar to the laser engineered net shaping (LENS) process [1]. It can be used to manufacture complex three-dimensional (3D) solid metallic parts directly from their computer aided design (CAD) files. This technology is gaining popularity because of its unique advantages, such as cost saving potentials and high cooling rates leading to fine microstructures [2,3].

During a LADMD process, a laser irradiation creates a melt region on the surface of a substrate. The powdery material is blown through a nozzle into the laser-induced melt pool to form a layer. After deposition of a layer, the nozzle and the laser beam assembly are raised vertically upward by a small increment. Then the next layer is built on the previous one. Thus a 3D part is built layer by layer from the bottom to the top [3–5].

LADMD is essentially a fusion and solidification process, which involves complicated interactions between the laser beam, metal powder and the substrate material. Typical physical phenomena in the LADMD process include laser-powder interactions, heat transfer, phase transformation, fusion, fluid flow, solidification and cooling. There are numerous variables which strongly influence the thermal behavior during the process, such as laser power, beam diameter, travel speed, powder feed rate, material properties (absorptivity, melting point, thermal conductivity, etc.), height increment per layer and initial substrate temperature. Some of these process parameters are strongly coupled to each other. So the dynamic process of the LADMD is a multivariable, strong coupling and time-varying process. Because the process is not yet fully understood, the selection of process parameters is often based on previous expe-

*Corresponding author (email: gyu@imech.ac.cn)

rience and trial experimentations. However, the desired quality and precision can be met only if the process parameters are carefully chosen on the basis of a thorough understanding of the physical phenomena involved.

During the LADMD process, the temperature field distribution plays an important role in obtaining better geometry accuracy and mechanical properties. The materials in each layer will undergo successive thermal cycles as new layers are added, so the thermal history of materials involves remelting and numerous lower temperature reheating cycling [6]. The molten materials have significantly effect on dimensional accuracy of the fabricated part. After several remelting cycles, the following consecutive thermal cycles of the materials can induce phase transformations which lead to progressive modification of microstructure and properties. Therefore, it is critical to understand the temperature history of the deposited materials [7–9].

Considering the large number of variables involved, systematic experimental investigations appear time-consuming for improving the process. Consequently, modeling becomes an efficient way to obtain necessary information or predict thermal fields induced during the LADMD process [5]. During the past decades, many analytical and numerical models have been developed by researchers to provide insights into the physical phenomena and predict the temperature distribution and phase transformations in the deposited part [5,6,10–15]. Kong et al. [11] developed a two-dimensional (2D) model of the transport phenomena occurring in the hybrid plasma-laser deposition manufacturing process. Qi and He et al. [10,15] presented a self-consistent 3D model for a coaxial laser powder cladding process. In these models, they used a level-set approach to track the free surface evolution of the melt pool and temperature field and fluid field were solved in a coupled manner. Since these comprehensive models computed the temperature, flow velocity and pressure and tracked the free surface of the melt pool, the computation was computationally expensive and complicated. Consequently, most other models were based on a heat transfer model with a necessary consideration of melting and solidification. Peyre et al. [5] proposed a three-step analytical and numerical approach to predict the shapes of manufactured structures and thermal history involved in the direct metal deposition (DMD) laser process. Zheng et al. [6] developed a 2D model to simulate the thermal history associated with the LENS process. Effects of the process parameters on the thermal history of deposited materials were also simulated and analyzed. Their model was simplified with the assumption that each deposited material in the melt pool is a thin metal disk. Yin et al. [12,14] developed 2D and 3D thermal models of the LENS process. They investigated the melt pool size, thermal history and cooling rate by the numerical simulation and experiments. The reliability of the 2D model was also evaluated by comparing the results obtained from the 2D and 3D models. Neela [13] developed a 3D model to simulate and analyze the thermal history as well as the effects of the processing parameters during the LENS process. In this model, the influence of the temperature-dependent material properties and latent heat were considered.

When the thermal history of deposited materials was determined, some properties of the fabricated part can be calculated and analyzed. Griffith et al. [9] measured temperature through inserted thermocouples during the fabrication of a H13 tool steel hollow box. They separated the thermal history into three different regions corresponding to the peak temperature, and then analyzed the microstructure evolution with the H13 phase diagram. Wang et al. [16] developed a 3D finite element model to predict the thermal history and residual stress field during the LENS process. Costa et al. [7] and Wang et al. [8] developed 3D finite element models to investigate the thermal history of materials and hardness distribution in the laser powder deposition process. Foroozmehr et al. [17] developed a finite element model coupled with a thermo kinetic model to predict the phase transformations of the laser deposition of AISI 4140 on a substrate with the same material. This model is similar to the model of Costa and Wang.

The majority of the above heat transfer models have neglected the influence of temperature-dependent material properties [6–8,12,14,16]. Often, the entire substrate, irrespective of its size, was forced to remain at ambient or some lower temperature throughout the deposition process, thereby imposing an unrealistic thermal boundary condition [7,12,18]. Despite numerous studies of the temperature field of the process, they all focused on the thermal history of the midpoints of each layer [6,12–14]. The characteristics of thermal history of the other points are still unclear. Moreover, the part was built by depositing a large number of layers during the fabrication process which caused a lot of thermal cycles. Most of the models reported simulated and analyzed only several layers [5,6,12–14]. What is the characteristic of thermal history during multilayer deposition and how to analyze the properties such as hardness through lots of thermal cycles have not been investigated in detail.

In this paper, a 3D transient finite element model was developed to study the temperature evolution during the multilayer LADMD process. A critical temperature specific to thermal history was defined to make the property analysis from thermal history easier. The distribution of it in the part was also discussed.

2 Finite element mathematical model

In this section, a 3D finite element model is developed to simulate the transient temperature field during the deposition of 50 consecutive layers of a thin-wall plate of SS316. Figure 1 shows a schematic diagram of the LADMD process with coaxial powder feeding.

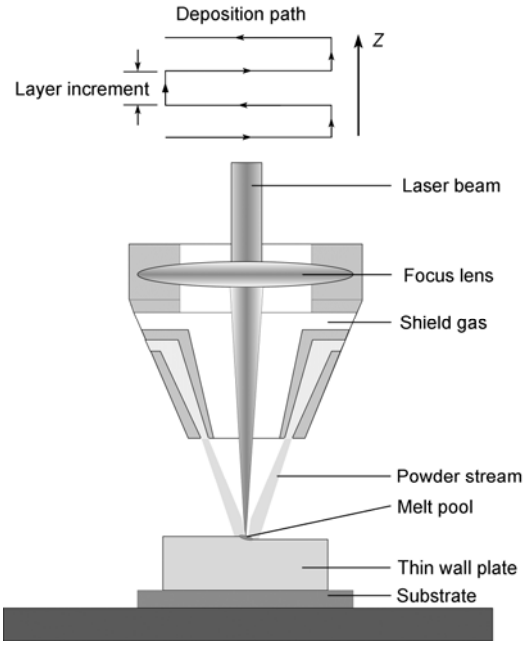

Figure 1 Schematic diagram of the LADMD process.

2.1 Governing equation

The transient temperature distribution $T(x, y, z, t)$ throughout the domain of the LADMD process can be obtained from the heat transfer equation with appropriate boundary conditions. The governing equation for the conservation of energy within computational domain is expressed as [19,20]:

$$\frac{\partial[\rho cT]}{\partial t}=\frac{\partial}{\partial x}\left[k\frac{\partial T}{\partial x}\right]+\frac{\partial}{\partial y}\left[k\frac{\partial T}{\partial y}\right]+\frac{\partial}{\partial z}\left[k\frac{\partial T}{\partial z}\right] \quad (1)$$

where ρ, c, t and k are density of the material, specific heat capacity, time and thermal conductivity, respectively.

2.2 Initial and boundary conditions

The initial temperature of the substrate is at room temperature. The powder particles are preheated and even melted by the laser during their flight to the melt pool. So the initial condition is

$$T(x,y,z)\big|_{t=0}=T_a, \quad (2)$$

where T_a is the room temperature. The convection and radiation boundary condition can be considered together as:

$$k(\nabla T\cdot\boldsymbol{n})\big|_S=\left[-h(T-T_a)-\varepsilon\sigma(T^4-T_a^4)\right]\big|_S \quad \text{if} \quad S\notin\Omega, \quad (3)$$

where $\boldsymbol{n}$ is the normal vector of the surface, ε is the emissivity, h is the heat convection coefficient, σ is the Stefan Boltzmann constant, S represents the work piece surface, Ω represents the area of the laser beam on the work piece. The effect of the moving laser beam can be considered as a surface heat source in the boundary conditions as follows:

$$k(\nabla T\cdot\boldsymbol{n})\big|_S=\left[aq-h(T-T_a)-\varepsilon\sigma(T^4-T_a^4)\right]\big|_S \quad \text{if} \quad S\in\Omega, \quad (4)$$

where a is the absorptivity, and q is the laser energy distribution on the work piece.

2.3 Assumptions

The 3D finite element model for the LADMD process was developed with the ANSYS parametric design language (APDL). The basic assumptions for the model are summarized as follows:

(1) The laser energy distribution is assumed to be a circular Gaussian TEM00 mode as follows:

$$q(r)=\frac{2Q}{\pi r_b^2}\exp\left(-\frac{2r^2}{r_b^2}\right), \quad (5)$$

where Q is the laser power, and r_b is the laser beam radius.

The powder particles absorb a portion of the laser energy; part of the remaining energy is absorbed by the work piece. For simplicity, it is assumed that the temperature of powder particles when reaching the melt pool is liquidus temperature. The thermal load of the work piece is given in the form of the average thermal flux density:

$$aq_m=\frac{a}{\pi r_b^2}\int_0^{r_b}q(r)2\pi r\mathrm{d}r=\frac{0.865aQ}{\pi r_b^2}, \quad (6)$$

where $q(r)$ is given by eq. (5).

(2) The radiation term in eqs. (3) and (4) makes the analysis highly non-linear. So for simplicity, a combined heat transfer coefficient (h_c) is used to simulate the effect of radiation and convection. It can be calculated from the relation as follows [20]:

$$h_c=2.41\times10^{-3}\varepsilon T^{1.61}. \quad (7)$$

The boundary condition can be expressed as follows:

$$k(\nabla T\cdot\boldsymbol{n})\big|_S=-h_c(T-T_a)\big|_S. \quad (8)$$

(3) Substrate preheating is often used to reduce the residual stress and the risk of thermal distortion and cracking. In practice, it is difficult to keep substrate temperature uniform and accurate. In this study, the substrate is preheated by laser beam scanning along the deposition path.

(4) At the bottom of the substrate, the adiabatic boundary condition is adopted.

(5) Since the LADMD process involves very rapid melting and solidification and the melt pool is small, the convective redistribution of heat within the melt pool is not significant. The vaporization of the metal and convective flow of heat, therefore, is not taken into account in the current study.

2.4 Model application

The material of powder and substrate used in the model is

SS316 whose chemical composition is given in Table 1. Some thermal properties and parameters used in this model are shown in Table 2. Due to lack of temperature-dependent thermal properties data in the liquid phase, an appropriate way at this stage of the analysis is to keep constant density and specific heat. Besides the enthalpy which is the integral of density times specific heat with respect to temperature is used to simulate the latent heat:

$$H = \int_{T_a}^{T} \rho(T)c(T)\mathrm{d}T. \tag{9}$$

At the solidus temperature (1643 K) the latent heat has been added to obtain the enthalpy value at the liquidus temperature (1673 K). Thus, the density, thermal conductivity, specific heat and enthalpy of SS316 are dependent on temperature, as described in ref. [22]. In real simulations, the effect of latent heat of fusion (melting or freezing) is considered by modifying the specific heat capacity which is evaluated from the enthalpy.

The geometry and finite element mesh used in the model are shown in Figure 2. The symmetric thin wall was fabricated by overlapping 50 single layers of material, each with a length of 51 mm, a thickness of 0.5 mm and a width of 3 mm. The thin wall is built on the surface of a substrate with 80 mm in length, 40 mm in width and 20 mm in thickness. The model is meshed with eight-node brick elements. The moving laser beam is simulated automatically using an APDL program to provide a heat flux boundary condition varying with time and location.

Table 1 Chemical composition of SS316 (wt %)

C	Si	Mn	P	S	Cr	Ni	Mo
0.08	1	2	0.045	0.03	18	14	3

Table 2 Parameter values used in the model

Parameter	Symbol	Value	Reference
Latent heat (J kg^{-1})	L	3×10^5	[21]
Solidus (K)	T_S	1643	[22]
Liquidus (K)	T_L	1673	[22]
Ambient temperature (K)	T_a	300	—
Emissivity	ε	0.62	[21]
Absorptivity	a	0.3	[18]
Radius of the laser beam (mm)	r_b	1.5	—

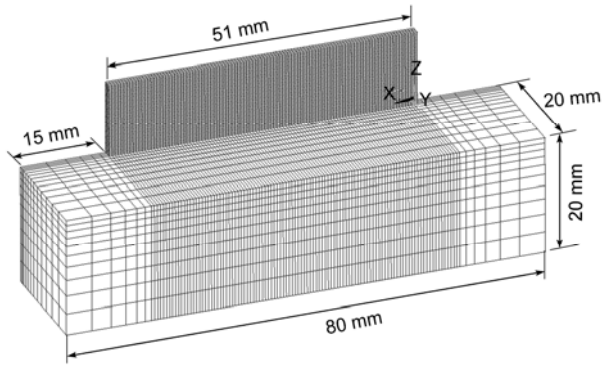

Figure 2 Finite element mesh and geometry for the thermal calculations of the LADMD process with 50 manufactured layers.

At the start, the initial node temperature of substrate is set to room temperature. All the elements of thin wall are inactive. In other words, they are not contributing to the solution. The substrate is preheated by laser radiation moving backwards and forwards several times along the deposition path. Then the deposition process begins. The continuous additions of metal powders are considered as successive discrete activation of a new set of elements in the computational domain at the beginning of each time step. The number of elements to be activated at each time step is determined from the volume of powder materials expected to enter the melt pool during that time step, which depends on the powder mass flow rate and scanning velocity. The boundary conditions are updated dynamically with the activation of new elements. When the 50 layers deposition process is finished, the substrate and thin wall cool down to room temperature naturally. The above calculations are implemented automatically using the APDL program. A flow chart showing the main steps of calculations in this study is presented in Figure 3.

3 Results and discussion

The experiments completed with LENS-deposited SS316 were made by Hofmeister et al. [9]. In these experiments, ultrahigh speed digital imaging techniques were employed to analyze the image of the melt pool and temperature gradient on the surface surrounding the melt pool. These experiments can be used to validate the model. The process parameters used are :the layer increment is 0.25 mm and travel speed of the laser beam is 7.65 mm/s. They both approximate to the conditions of Hofmeister's experiments. The average power density applied on the area of the laser beam on the part is 27.55 W/mm^2. Then the calculated result of the melt pool temperature profile in the center of the tenth layer and experimental data are shown in Figure 4. The horizontal line in the figure indicates the liquidus temperature of SS316 (1673 K) and meets both the computed and the corresponding measured temperature profiles at their point of intersection, which indicates that the computed and the corresponding measured the melt pool radius is about 1 mm. Away from the melt pool, deviation is found between the computed and measured temperatures which may have resulted from the difference of some other process parameters such as the laser power absorbed by the materials and substrate temperature. The calculated temperature profile is in reasonable agreement with the experimental results measured, which possibly supports the

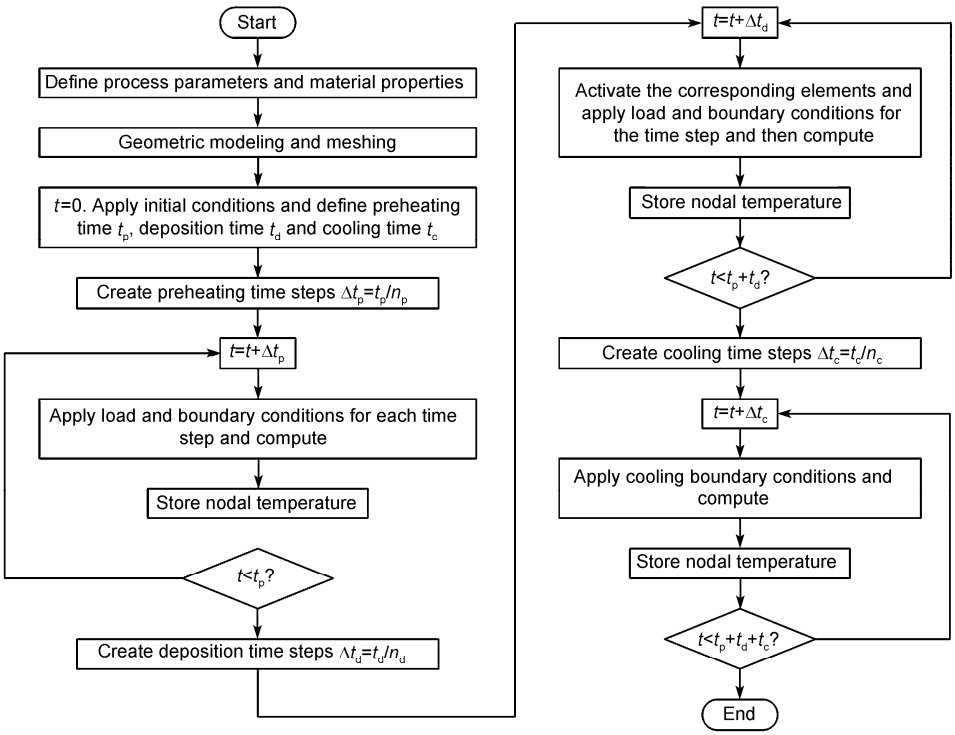

Figure 3 Flow chart showing the main steps of calculation involved in the model.

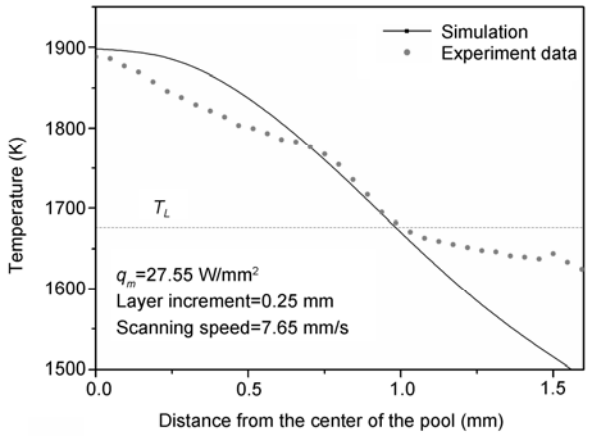

Figure 4 Comparison of the computed results and the corresponding experimentally measured results.

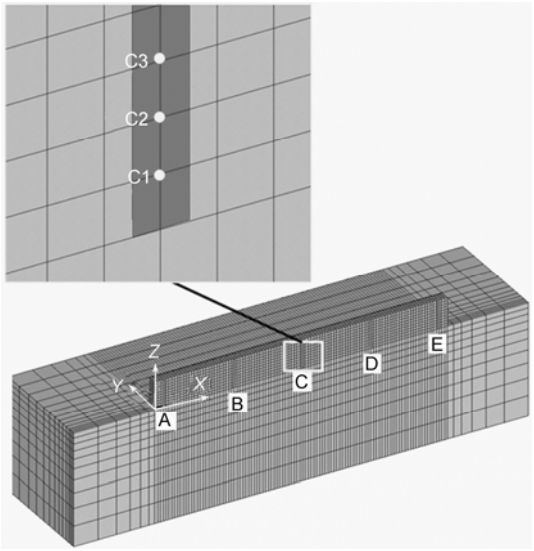

Figure 5 Sketch of representative points of the thin wall used in thermal history analysis.

numerical model to be used further to study the characteristics and disciplines of the thermal history during the LADMD process.

In order to analyze the characteristics of thermal history at different locations of the part, the points in the plane y=0 are selected as shown in Figure 5. Location A and location E are two ends of the laser beam's movement along the x axis. Location B, location C and location D are distributed evenly between A and E. The X axis coordinate values of A, B, C, D, E are 1.5, 13.5, 25.5, 37.5 and 49.5 mm, respectively (laser beam radius=1.5 mm). Points at different locations are expressed with a number matching a location letter indication. The number following the letter represents the layer number. For example, C2 denotes the midpoint of the second layer. Thus, we study the thermal history characteristics of the part by the means of comprehensive investigation and analysis of thermal histories of material at these representative points.

The deposition parameters used are: scanning speed is 3 mm/s, layer increment is 0.5 mm and average power

density is 27.55 W/mm^2. The thermal histories calculated of the five representative points of the fifth layers are shown in Figure 6. It can be seen that thermal history is formed by consecutive thermal cycles caused by successive layer deposition. The thermal histories of point A5, C5, and E5 consist of single-peak thermal cycles. The initial thermal history of point B5 and point D5 consists of double-peak thermal cycles. This is because laser beam passed over locations B and D two times in one cycle. When the deposited materials atop the fifth layer reach a certain thickness, double-peak effect is not clear and the double-peak even becomes single-peak gradually. Period of thermal cycle of all the points except point C5 is the time for the laser round-trip time while the period of thermal cycle of point C5 is a half. This is caused by the deposition path. Only the interval between scanning over location A, location C and location E is the same. Although the characteristics of the thermal cycles at different locations are not all the same, the thermal history can be treated as a series of discrete thermal cycles in the analysis.

Figure 7 shows the computed thermal histories of deposited materials at locations A, B, C of layers 1, 5, and 10. It is observed that the thermal history of the same location at each layer is very similar. They are all formed by one and one consecutive thermal cycle and share the same changing trend. In each thermal cycle, the temperature reaches a peak every time the laser beam passes over the correspond location of the part, and then decreases to a minimum value before the laser beam starts scanning the location of a new layer. Fluctuations of the temperature tend to dampen as more layers are deposited. The peak temperature falls continually as the building height increases and the laser beam also moves up. However, the resident temperature of each thermal cycle increases continually as the deposited materials atop it increase. When the part is finished, the temperature cools down to the room temperature slowly.

Figure 8 shows the thermal history and corresponding cooling rate at the midpoint of the first layer. This point experienced fifty thermal cycles before cooling down to room temperature. It can be observed that the peak temperatures of initial two thermal cycles are both higher than the liquidus temperature. In other words, materials of a layer are remelted when the next layer is deposited. We also

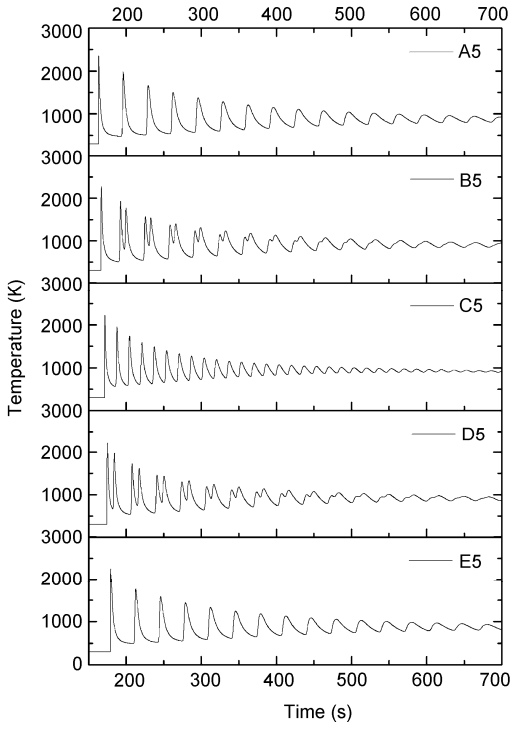

Figure 6 Thermal histories at different points of the 5th layer.

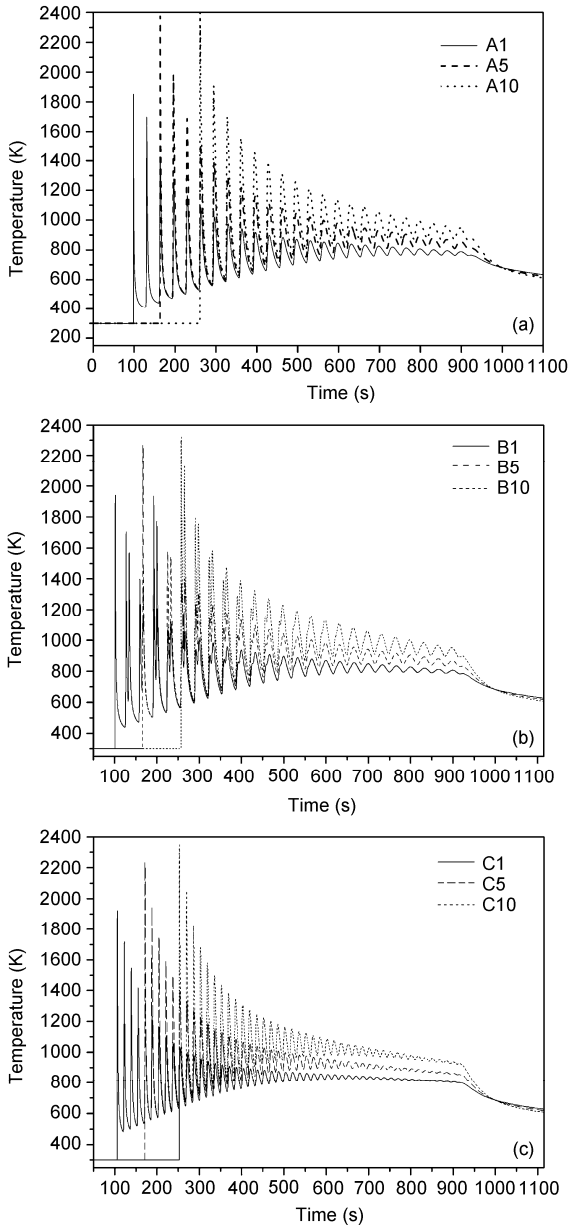

Figure 7 Thermal histories of the representative points of layers1, 5 and 10.

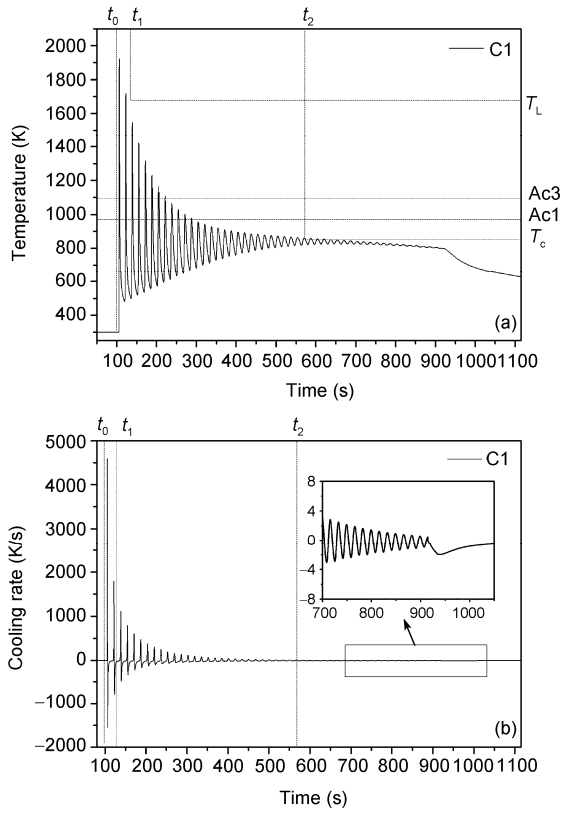

Figure 8 Thermal history (a) and corresponding dT/dt (b) at the midpoint of the first layer.

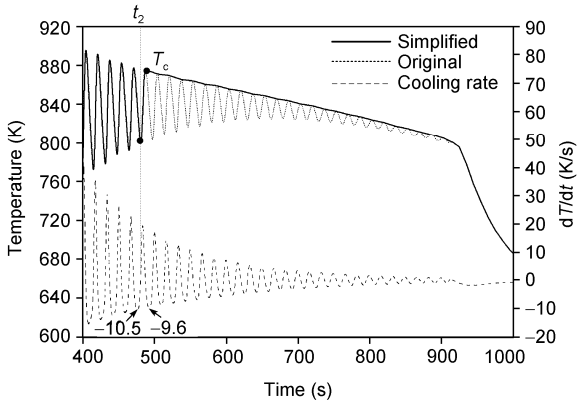

Figure 9 Sketch of the simplification of the thermal history.

know that the layer increment is 0.5 mm. So it can be deduced that the depth of the melt pool is approximately 1–1.5 mm. During the initial stage, the deposited materials experience a significant rapid quenching effect and can attain a very high cooling rate of 10^3 K/s. The maximum cooling rate for each thermal cycle decreases as more layers are deposited, which is due to the integrated heat of the substrate and new layers. After the deposited materials reach a certain thickness, the rapid quenching effect decreases and even disappears. Figure 8(b) clearly shows that the maximum cooling rate is approximately 2 K/s when the materials cool down to room temperature. Here, 10 K/s is chosen as a critical cooling rate which is of the same order of magnitude of the maximum cooling rate when the part is cooling down to the room temperature. When the maximum cooling rate of one cycle in thermal history is larger than or equal to 10 K/s and the next one is less than 10 K/s, we define the maximum temperature and start time of the next cycle as important parameters T_c and t_2 respectively, as shown in Figure 9.

As shown in Figure 8, t_0 is the start time of the first thermal cycle of thermal history and t_1 is the end time of the last thermal cycle whose maximum temperature is above the liquidus temperature. Then the thermal history can be separated into three different regions corresponding to the peak temperature and cooling rate. The first region (t_0–t_1) is composed of several thermal cycles whose maximum temperatures are larger than the liquidus temperature. In these thermal cycles, materials undergo melting and solidification and remelting process from which we can deduce the depth of the melt pool approximately. The second region (t_1–t_2) is composed of a series of thermal cycles whose maximum cooling rate is larger than 10 K/s. The third region is from t_2 to the end time. Because the maximum cooling rate of thermal cycles in this region is less than 10 K/s, the temperature fluctuations of these thermal cycles can be neglected. It can be treated as the temperature cooling down from one peak to the other peak linearly. Thus this region can be treated as one thermal cycle whose peak temperature is T_c and then cools down to room temperature monotonically. The simplification makes the analysis or calculation of properties from the thermal history easier. No matter how many layers deposited and thermal cycles included in the thermal history, we just need to analyze the thermal cycles between t_0 and t_2 and then analyze the last simplified thermal cycle whose peak temperature is T_c.

It can be concluded that T_c has significant influence on microstructure evolution and properties of the built part. Figure 10 shows the value of T_c at the center line of layers 1, 3, and 5 along the laser travel direction. Lower T_c at both ends of the plate and higher T_c inside the plate are observed. Therefore, it is possible that microstructure in the same layer is different. Locations A and E are two ends of the laser beam's movement along the x axis. So the lower T_c at locations A and E comes from more thermal energy is dissipated due to radiation and convection. There is also a local minimum of T_c at the midpoint of each layer. This is because a short time interval of laser irradiations allows less thermal energy to be dissipated. We can also see that T_c increases with the deposited layer, chiefly because that laser energy absorbed in the part is more than the surface heat loss. As more layers are deposited, the energy accumulates and the whole temperature of the part increases. The distribution variation of T_c shows why the final part presents nonuniform microstructure and properties. Good properties of

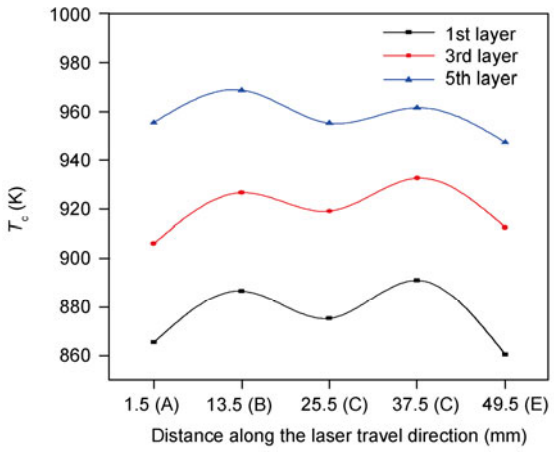

Figure 10 (Color online) Distribution of T_c along the laser travel direction.

the final part cannot be obtained by using invariable process parameters during the LADMD process. Real time thermal signature should be used as a feedback mechanism, and then the process parameters such as laser power can be adjusted to make sure that the temperature is in the predefined range during the process.

4 Conclusion

A 3D transient numerical model was developed for the multilayer LADMD process. The main conclusions of the present work are as follows:

(1) All the thermal histories of the deposited materials of the part are similar. It can be considered as a sequence of thermal cycles. During the initial stage, the deposited materials experience a significant rapid quenching effect and can attain a very high cooling rate of 10^3 K/s. Then the peak temperature of thermal cycle decreases and the resident temperature increases continually as the subsequent layer atop it increases. When the deposited materials above reach a certain thickness, the rapid quenching effect decreases and even disappears. The thermal history can be simplified according to the peak temperature and cooling rate of each cycle involved. The temperature fluctuation of thermal cycles with a low cooling rate can be neglected. Thermal cycles with a low cooling rate can be treated as one thermal cycle, which makes the analysis and calculation easier.

(2) The LADMD process is a complex time-varying system. The temperature of deposited materials constantly increases with deposition because of laser energy accumulation from the beginning. The thermal history of the deposited materials which is dependent on the process parameters has significant influences on the geometric precision and mechanical properties of the final part. Thus better properties can be obtained by maintaining a predetermined steady melt pool temperature field, which requires time-varying process parameters according to the real-time temperature feedback.

This work was supported by the National Natural Science Foundation of China (Grant No. 10832011).

1 Dinda G P, Dasgupta A K, Mazumder J. Laser aided direct metal deposition of inconel 625 superalloy: Microstructural evolution and thermal stability. Mater Sci Eng A, 2009, 509(1-2): 98–104
2 Mazumder J, Choi J, Nagarathnam K, et al. The direct metal deposition of H13 tool steel for 3-D components. J Miner Metal Mater Soc, 1997, 49(5): 55–60
3 Pinkerton A J, Li L. An analytical model of energy distribution in laser direct metal deposition. Proc Inst Mech Eng B-J Eng Manuf, 2004, 218(4): 363–374
4 Ye R Q, Zhou Y Z, Wei W, et al. Numerical modeling of the thermal behavior during the LENS process. Mater Sci Tech, 2003: 369–376
5 Peyre P, Aubry P, Fabbro R, et al. Analytical and numerical modelling of the direct metal deposition laser process. J Phys D-Appl Phys, 2008, 41(2): 025403
6 Zheng B, Zhou Y, Smugeresky J E, et al. Thermal behavior and microstructural evolution during laser deposition with laser-engineered net shaping: Part I. Numerical calculations. Mater Sci Eng A, 2008, 39A(9): 2228–2236
7 Costa L, Vilar R, Reti T, et al. Rapid tooling by laser powder deposition: Process simulation using finite element analysis. Acta Mater, 2005, 53(14): 3987–3999
8 Wang L, Felicelli S. Process modeling in laser deposition of multilayer SS410 steel. J Manuf Sci Eng, 2007, 129(6): 1028–1034
9 Griffith M L, Ensz M T, Puskar J D, et al. Understanding the microstructure and properties of components fabricated by laser engineered net shaping. Mater Res Soc, 2000, 625: 9–20
10 Qi H, Mazumder J, Ki H. Numerical simulation of heat transfer and fluid flow in coaxial laser cladding process for direct metal deposition. J Appl Phys, 2006, 100(2): 024903
11 Kong F R, Zhang H O, Wang G L. Numerical simulation of transient multiphase field during hybrid plasma-laser deposition manufacturing. J Heat Transfer, 2008, 130(11): 112101
12 Yin H, Wang L, Felicelli S D. Comparison of two-dimensional and three-dimensional thermal models of the lens process. J Heat Transfer, 2008, 130(10): 102101
13 Neela V, De A. Three-dimensional heat transfer analysis of LENS process using finite element method. Int J Adv Manuf Technol, 2009, 45(9–10): 935–943
14 Wang L, Felicelli S D, Craig J E. Experimental and numerical study of the LENS rapid fabrication process. J Manuf Sci Eng, 2009, 131(4): 041019
15 He X, Mazumder J. Transport phenomena during direct metal deposition. J Appl Phys, 2007, 101(5): 053113
16 Wang L, Felicelli S D, Pratt P. Residual stresses in lens-deposited Aisi 410 stainless steel plates. Mater Sci Eng A, 2008, 496(1-2): 234–241
17 Foroozmehr E, Kovacevic R. Thermokinetic modeling of phase transformation in the laser powder deposition process. Metall Mater Trans A, 2009, 40A(8): 1935–1943
18 Wang L, Felicelli S, Gooroochurn Y, et al. Optimization of the lens (R) process for steady molten pool size. Mater Sci Eng A, 2008, 474(1-2): 148–156
19 Holman J. Heat Transfer. Beijing: China Machine Press, 2002
20 Alimardani M, Toyserkani E, Huissoon J P. A 3d dynamic numerical approach for temperature and thermal stress distributions in multilayer laser solid freeform fabrication process. Opt Lasers Eng, 2007, 45(12): 1115–1130
21 Wang L, Felicelli S. Analysis of thermal phenomena in lens (Tm) deposition. Mater Sci Eng A, 2006, 435: 625–631
22 Capriccioli A, Frosi P. Multipurpose ANSYS FE procedure for welding processes simulation. Fusion Eng Des, 2009, 84: 546–553